Driven kinks in the anharmonic Frenkel-Kontorova model

O. M. Braun,[1,*] Hong Zhang,[2] Bambi Hu,[2,3] and J. Tekic[2]
[1]*Institute of Physics, National Ukrainian Academy of Sciences, 03650 Kiev, Ukraine*
[2]*Department of Physics and Centre for Nonlinear Studies, Hong Kong Baptist University, Hong Kong*
[3]*Department of Physics, University of Houston, Houston, Texas 77204-5505, USA*
(Received 2 December 2002; published 6 June 2003)

Multiple and supersonic topological excitations (kinks) driven by an external dc force in the Frenkel-Kontorova model (a chain of atoms subjected to a periodic substrate potential) with the exponential interatomic interaction are studied with the help of numerical simulation. The simulation results are interpreted in terms of dynamics of two limiting cases, the exactly integrable sine-Gordon equation and the Toda chain. The stability of driven kinks and scenarios of their destruction are described for a wide range of model parameters.

DOI: 10.1103/PhysRevE.67.066602 PACS number(s): 45.05.+x, 63.20.Ry, 05.60.−k

I. INTRODUCTION

Nonequilibrium dynamics of simple systems of interacting particles subjected to an external periodic potential, damping, and driven by an external force, is a very rich and interesting theoretical problem, as well as having many important applications in such areas as mass transport, conductivity, tribology, Josephson transmission lines, etc. In these systems the mass or charge transport is carried out by topological excitations, the so-called kinks that describe a local compression (or expansion in the case of antikink) of the chain. A classical example of these type of systems is the exactly integrable sine-Gordon (SG) equation, where the kink has the following form:

$$u_l(t) = 4 \arctan \exp[\mp(la - v_{\mathrm{kink}}t)/d]. \tag{1}$$

Here, u_l describes the shift of the lth atom from a minimum of the substrate potential

$$V_{\mathrm{sub}}(x) = \frac{1}{2}\varepsilon[1-\cos(2\pi x/a)] \tag{2}$$

of the height $\varepsilon = 2$ and period $a = 2\pi$ (throughout this paper we use dimensionless system of units and assume that the atomic mass $m_a = 1$), v_{kink} is the kink velocity, $d = (a\sqrt{g})\sqrt{1-v_{\mathrm{kink}}^2/c^2}$ is its width, $c = a\sqrt{g}$ is the sound speed in the chain of atoms harmonically interacting with the elastic constant g, and the signs $\mp$ correspond to kink and antikink configurations, respectively. The SG kink may be considered as a quasiparticle with the effective mass $m(v_{\mathrm{kink}}) = (2/\pi^2\sqrt{g})/\sqrt{1-v_{\mathrm{kink}}^2/c^2}$, which moves freely through the system. In the discrete SG model (the well-known Frenkel-Kontorova model, e.g., see Ref. [1], and references therein), however, the motion of the 2π kink is subjected to an effective Peierls-Nabarro (PN) periodic potential and, thus, the kink radiates phonon and loses its kinetic energy during motion. Therefore, to keep the kink moving, one has to apply an external dc force f, so that the motion equation takes the following form:

$$\ddot{u}_l(t) + \eta\dot{u}_l(t) + \sin u_l - V'(u_{l+1} - u_l + a) + V'(u_l - u_{l-1} + a) = f, \tag{3}$$

where the dot stands for the time derivative, η is the coefficient of the external viscous damping, which models the energy exchange between the chain and the substrate, and the interaction between the atoms, $V(x)$, is assumed to be purely harmonic in the classical Frenkel-Kontorova model, $V(x) = \frac{1}{2}g(x-a)^2$.

The SG kinks of the same topological charge repel one another. Therefore, the steady-state solution of the driven SG system should correspond to either a single moving kink (the 2π kink with the topological charge $p = 1$) or a train of equidistant kinks (the so-called cnoidal wave). In the *discrete* SG model, on the contrary, *multiple* kinks with the topological charge $p \geqslant 2$ may also exist. This fact was first observed by Peyrard and Kruskal [2] in numerical simulation. It was found that a ballistic motion of 4π and 6π kinks in the classical FK model is possible, if the elastic constant g exceeds some critical value g_p (where $g_p \ll 1$), and the velocity of these multiple kinks has to have a certain value that increases with g. Later, the ballistic motion of the $p = 2$ kink was studied numerically by Savin *et al.* [3] with the help of the pseudospectral method, where a hierarchy of the double kink states characterized by different distances between two single kinks was found. Each of these bound states is dynamically stable for a certain (preferred) value of the velocity given by a set of model parameters.

A qualitative explanation of existence of multiple kinks was given by Malomed [4] (see also a more recent paper by Ustinov *et al.* [5]). Due to the discreteness effects, the ''forward'' 2π kink of the multikink configuration emits a strong radiation behind itself, which helps the kinks immediately following it to overcome the PN barriers. Thus, the multiple kinks are stable due to ''compensation'' of the waves emitted by single kinks when these waves happen to be out-of-phase and suppress each other. A more rigorous explanation was

*Electronic address: obraun@iop.kiev.ua

given later by Champneys and Kivshar [6]. Due to the discreteness effects, the motion equation of the FK model in the quasicontinuum approximation reduces to a perturbed SG equation with a fourth-order dispersion term. Without the driving and damping, $f=\eta=0$, the propagating 2π kink solution does not exist at all; the single kink is always pinned by the PN potential. At the same time, the motion equation has four analytical solutions for the double-kink boundary condition. One of these solutions corresponds to the 4π-kink propagating with the fixed velocity v_2 ($v_2/c=\sqrt{2/3}\approx 0.82$ for $g=1$), while three other solutions describe ''excited'' states of the double kink and are characterized by lower velocities. Besides, there also exist solutions with higher topological charges.

Motion of the double kink in the *driven* underdamped FK model was studied numerically by Ustinov *et al.* [5]. They observed four ''bunched'' states of two single kinks, which differ by the number of the oscillations trapped between the two 2π kinks. Such ''resonant'' states exist for certain intervals of the driving force, which overlap. At the lower boundary of these intervals, the velocity of the double kink is very close to that calculated by Champneys and Kivshar [6]. The driven FK model was also studied in a series of papers by Braun *et al.* [7–10], where the existence of multiple kinks was observed as well. In the SG model, however, the topological excitations are always subsonic, the kink cannot propagate with a velocity $v_{\rm kink}$ larger than the sound speed c because of Lorentz contraction of kink's width. Moreover, in the discrete FK chain, the kink decays even earlier, at a velocity $v_{\rm crit}<c$, because of a strong radiation of phonons in the kink's tail [10].

However, in the generalized FK model, where the interatomic interaction is *anharmonic*, the kink may reach a supersonic velocity $v_{\rm kink}>c$ (e.g., see Refs. [8,11], and references therein). A limiting case of the discrete anharmonic model is the exactly integrable Toda chain [12], where the substrate potential is totally absent, while the adjacent atoms interact via exponential law

$$V(x)=\frac{\alpha}{\beta}\exp[-\beta(x-a_0)]+\alpha(x-a_0). \tag{4}$$

Expanding $V(x)$ into Taylor series for small $(x-a_0)$, we obtain $V(x)\approx\alpha/\beta+\frac{1}{2}(\alpha\beta)(x-a_0)^2[1-\frac{1}{3}\beta(x-a_0)]$. Thus, at a small deviation of the interatomic distances from the equilibrium distance a_0, $|x-a_0|\ll\beta^{-1}$, the Toda potential is close to the harmonic potential with the elastic constant $g=\alpha\beta$. For the higher deviations, a measure of nonlinearity of interaction is determined by the anharmonicity parameter β, and in the limit $\beta\to\infty$ the Toda potential reduces to the hard-core potential. The Toda chain allows the existence of a *dynamical* soliton, which has the following form:

$$u_l=\frac{1}{\beta}\ln\left(\frac{1+\exp\{2\mu[(l-1)a_0-v_{\rm Toda}t]\}}{1+\exp[2\mu(la_0-v_{\rm Toda}t)]}\right), \tag{5}$$

where u_l describes now the displacement of the lth atom from the equilibrium position $x_{l0}=la_0$. The parameter μ in Eq. (5) is coupled with the soliton velocity $v_{\rm Toda}$ by the relationship $v_{\rm Toda}=c\sinh(\mu a_0)/(\mu a_0)$, and $c=a_0\sqrt{g/m_a}$ is again the sound velocity in the chain. The Toda soliton is a one-parameter dynamical soliton localized within a region $\sim\mu^{-1}$. It is characterized by the effective mass $m(v_{\rm Toda})=2\mu(v_{\rm Toda})/\beta$ and describes a local compression of the chain characterized by a jump of displacement $\Delta u\equiv u_{+\infty}-u_{-\infty}=-2\mu a_0/\beta$, which continuously depends on the soliton velocity. Note that the dynamical soliton must move with the supersonic (faster-than-sound) velocity $v_{\rm Toda}>c$, because in the limit $v_{\rm Toda}\to c$ the soliton width tends to infinity and the soliton disappears. Note also that the Toda soliton cannot be driven by a dc force. Because the system is spatially homogeneous, the external force f will induce a drift of all chain's atoms with the same velocity $v=f/\eta$.

If the Toda chain is disturbed, e.g., by the substrate potential (2), the system becomes nonintegrable and the soliton should disappear because of phonon radiation. In the present paper, we will discuss the commensurate situation only, when $a_0=a=2\pi$. In the presence of the external substrate potential due to boundary conditions at infinity, the ''jump'' Δu must be equal to pa with p being an integer. Thus, one may expect the existence of multiple solitons with a topological charge $p\geqslant 1$, if the width of the Toda soliton matches with the period of the substrate potential. For the p kink, we obtain $2\mu=p\beta$ or

$$\frac{v_{\rm Toda}}{c}=\frac{\sinh(\pi\beta p)}{\pi\beta p}. \tag{6}$$

For example, for the anharmonicity parameter $\beta=1/\pi$, we have $v_{\rm Toda}/c=(\sinh p)/p\approx 1.18$ for the 2π kink (a single kink, $p=1$), $v_{\rm Toda}/c\approx 1.81$ for the 4π kink (the double kink, $p=2$), and $v_{\rm Toda}/c\approx 3.34$ for the 6π kink (the triple kink, $p=3$), correspondingly. Thus, the supersonic and multiple kinks may be treated as Toda solitons ''disturbed'' by the external periodic potential.

Supersonic topological solitons, which move almost without radiation, were first observed by Bishop *et al.* [13] in molecular dynamics study of polyacetylene. Then, the supersonic kinks were studied by Savin [14] in the framework of the ϕ^4 model with anharmonic interatomic interaction. Later, Zolotaryuk *et al.* [15] have studied numerically with the help of the pseudospectral method the ballistic supersonic kinks of different topological charges in the framework of the FK model with exponential interatomic interaction. It was found that the multiple kink exhibits a hierarchy of ''excited'' states, $n=1,2,\ldots,n_{\rm max}$, which may be considered as n acoustic Toda solitons bounded together, when the sum of their amplitudes coincides with the period of the substrate potential. All these solutions were found to be dynamically stable and propagate with their own preferred velocities.

The goal of the present work is a detailed study of kink propagation in the *anharmonic driven* FK model. Indeed, now the Toda soliton may be driven by the external force, because the atoms far away from the soliton are pinned at the minima of $V_{\rm sub}(x)$, provided the force is not too large, $|f|<\varepsilon/2=1$. The driven kinks were already considered in our previous papers [7–11]. Now, however, we present a much

more detailed study of the problem for a wide range of model parameters. In particular, *we determine the intervals of forces and kink's velocities where the kinks are stable.* We show that these intervals may *overlap* for some sets of model parameters, while in other cases there may exist *forbidden gaps* where no stable kinks exist. Then, *we describe scenarios of kink destruction* when the force goes outside the stability interval. When the stability intervals overlap, we also study *collisions of kinks of different types.*

Most of our results were obtained with the help of numerical solution of the motion equation (3) with the substrate potential (2), the interatomic interaction (4), and periodic boundary conditions. The simulation was typically performed for the chain of $N=2000$ atoms with the help of the Runge-Kutta method. A special attention has to be given to the initial configuration. In the case of the single kink, one may start from the static SG kink and then slowly increase the dc force (typically with a step $\Delta f=0.001$–0.005). At each step, the steady state was found with the help of the procedure described in detail in our previous paper [10]. For the double or triple kink, however, we have to start from the moving kink configuration, because these kinks do not exist in the static state. In these cases, we started from the Toda kink configuration and guessed the initial value of the dc force leading to a stable kink motion. Then, the force increased and decreased adiabatically until the stability interval was found. Similarly, to find the kink shape for different values of the model parameters η, g, or β, we started from the known configuration and then changed the corresponding parameter adiabatically.

The paper is organized as follows. The simulation results are presented in Sec. II. Then, in Sec. III, we give a qualitative explanation of kink behavior observed in simulation. Finally, Sec. IV concludes the paper.

II. SIMULATION

In Fig. 1 we present the simulation data for the case of $g=1$ and $\beta=1/\pi$ for three different values of the damping coefficient: $\eta=0.012$, 0.024, and 0.05. For $\eta=0.012$, the 2π kink is stable for forces $f<f_{1r}\approx 0.29$, the 4π kink exists for forces within the interval $f_{2l}<f<f_{2r}$, where $f_{2l}\approx 0.14$ and $f_{2r}\approx 0.33$, and the 6π kink is stable for forces $f_{3l}<f<f_{3r}$ with $f_{3l}\approx 0.42$ and $f_{3r}\approx 0.67$. In the case of $\eta=0.024$, we obtained $f_{1r}\approx 0.372$ for the single kink, $f_{2l}\approx 0.253$ and $f_{2r}\approx 0.579$ for the double kink, and $f_{3l}\approx 0.915$ for the triple kink (the right boundary is not determined in this case). Finally, for $\eta=0.05$, we found $f_{1r}=0.5067$ for the single kink, and $f_{2l}=0.4688$ and $f_{2r}=0.8767$ for the double kink. The triple kink does not exist for this value of the damping coefficient, because the kink cannot reach the necessary velocity for forces $f<1$.

Next, we checked the system behavior for different values of the elastic constant g. In particular, for the parameter set $g=0.5$, $\beta=1/\pi$, and $\eta=0.012$, we found that the 2π kink is stable for $f<f_{1r}\approx 0.27$, the 4π kink is stable for forces within the interval $f_{2l}<f<f_{2r}$ with $f_{2l}\approx 0.1$ and $f_{2r}\approx 0.28$, and the 6π kink is stable for forces $f_{3l}<f<f_{3r}$ with $f_{3l}\approx 0.305$ and $f_{3r}\approx 0.52$. Figure 2 shows these data as com-

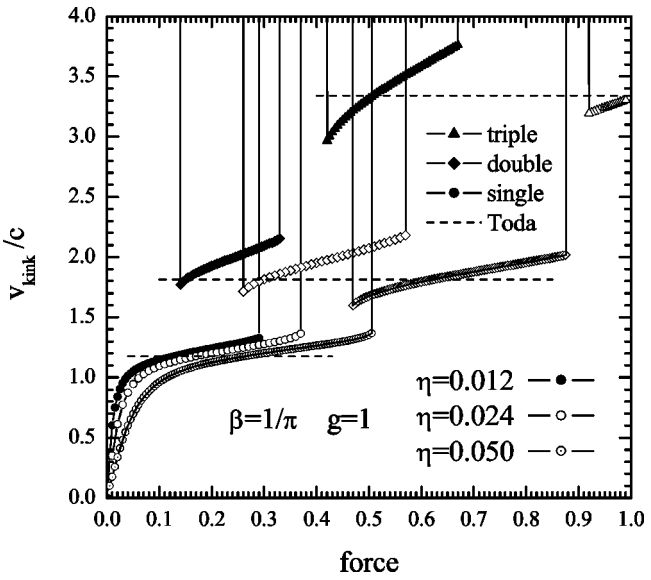

FIG. 1. Dependence of the kink velocity $v_{\rm kink}$ (normalized on the sound speed $c=a\sqrt{g}$) on the dc force f for the single kink (circles), double kink (diamonds), and triple kink (triangles) for three values of the damping constant: $\eta=0.012$ (solid symbols), $\eta=0.024$ (open symbols), and $\eta=0.05$ (open dotted symbols). Other parameters are $\beta=1/\pi$, $g=1$, and $N=2000$. The dashed horizontal lines show the velocity of the corresponding Toda soliton given by Eq. (6). The solid vertical lines indicate the transition from the steady kink motion to the totally running state with all the atoms moving with the velocity $\approx f/\eta$.

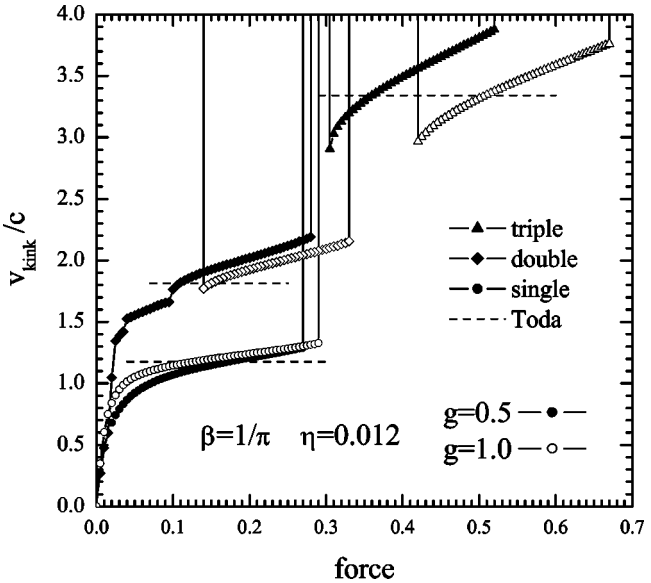

FIG. 2. Dependence $v_{\rm kink}(f)/c$ for the single kink (circles), double kink (diamonds), and triple kink (triangles) for two values of the elastic constant: $g=0.5$ (solid symbols) and $g=1$ (open symbols). Other parameters are $\beta=1/\pi$ and $\eta=0.012$. The dashed horizontal lines show the velocities of the corresponding Toda soliton, while the solid vertical lines describe the transitions to the running state.

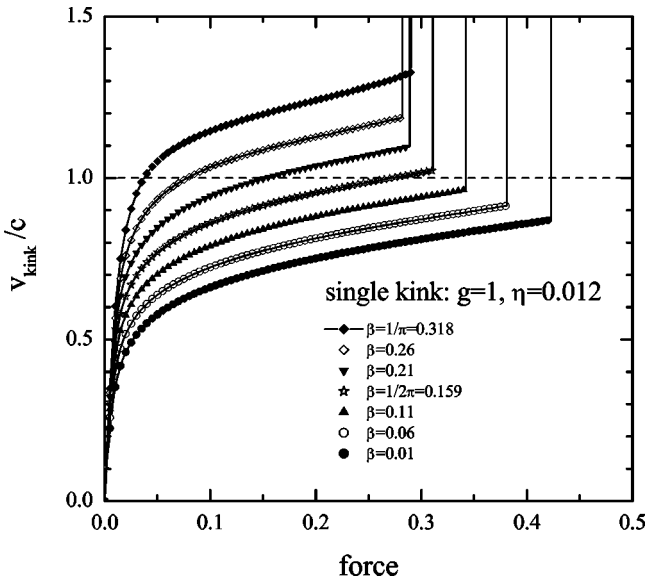

FIG. 3. Velocity v_{kink}/c vs the force f for the single kink for different values of the anharmonicity parameter β indicated in the legend ($g=1$ and $\eta=0.012$).

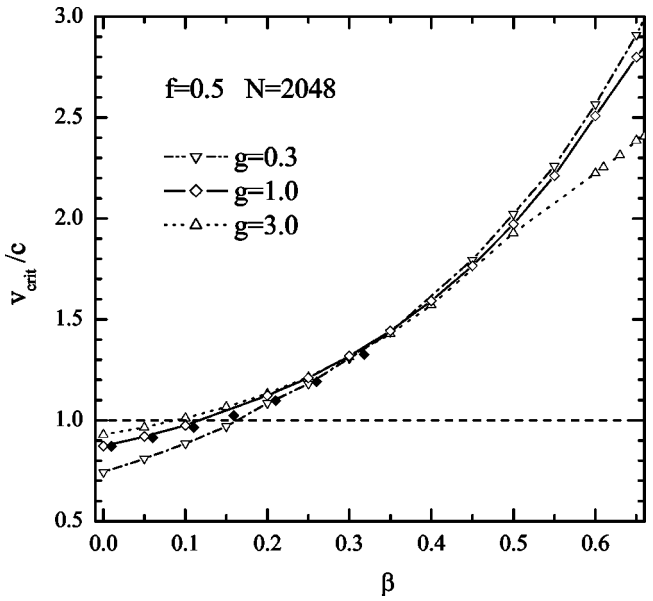

FIG. 4. Critical velocity v_{crit}/c as a function of the anharmonicity parameter β for the single kink at the fixed force $f=0.5$ and three different values of the elastic constant g: $g=0.3$ (down triangles), $g=1$ (open diamonds), and $g=3$ (triangles). The critical velocity for the constant damping $\eta=0.012$ extracted from Fig. 3 is also shown by solid diamonds.

pared to the $g=1$ case. One can see that the $v_{\mathrm{kink}}(f)$ dependencies for these two values of the elastic constant are very similar (except the left boundary of the double kink as will be discussed below in Sec. II B).

When the dc force adiabatically changes within the stability interval, the $v_{\mathrm{kink}}(f)$ dependence does not exhibit hysteresis, the kink velocity is uniquely defined by the force. However, the system exhibits a ''trivial'' hysteresis; if the system goes to the running state, for example, when the force increases above f_{pr}, this state remains unchanged if the force decreases back to lower values. In the same way, when the double kink splits into two single kinks during force decreasing process at $f<f_{2l}$, the two kinks continue to move being separated, and do not unite again into the double kink when the force increases above f_{2l} (see Ustinov *et al.* [5]).

The described results already allow us to make the following conclusions: (1) driven supersonic kinks do exist; (2) multiple kinks also exist in the driven system; (3) the multiple kinks cannot be static; when the kink velocity decreases below a certain value, the multiple kink either splits into separate single kinks, or the system goes to the running state; (4) the stability intervals of multiple kinks may overlap (e.g., $f_{1r}>f_{2l}$ for the parameter values used in Fig. 1); (5) on the other hand, there may exist forbidden gaps where no kinks are stable (e.g., $f_{2r}<f_{3l}$ as in Fig. 1); (6) the comparison of the results for different values of the damping constant suggests that the main factor, which determines the kink stability, is its velocity.

Below, we will check these conclusions in detail as well as study the mechanisms of the kink decay.

A. Single kink

As was mentioned above, the supersonic kinks could be expected for the anharmonic FK model only. Indeed, in Fig. 3, we present the simulation results for the single kink for $g=1$, $\eta=0.012$, and different values of the anharmonicity parameter β. One can see that the kink can reach a supersonic velocity $v_{\mathrm{kink}}>c$ before it becomes unstable at $v_{\mathrm{kink}}=v_{\mathrm{crit}}$ only for a large enough value of β (e.g., when $\beta \geqslant 1/2\pi$ for the parameters used in Fig. 3).

The critical velocity of the single kink extracted from the data of Fig. 3 is shown by solid diamonds in Fig. 4. As follows from Fig. 1, the critical velocity does not depend essentially on the damping constant η. This allows us to use the following algorithm proposed first in Ref. [9]. Starting from the kink configuration at a fixed force f and large enough damping η, we slowly decrease η until the kink becomes unstable and the system goes to the running state with all the atoms moving with approximately the same velocity f/η. The simulation results obtained in this way are presented in Fig. 4 for three different values of the elastic constant g ($g=0.3$, 1, and 3). One can see that supersonic velocities are observed for $\beta>0.1$–0.2 only. At the same time, the shape of the static kink does not change essentially from that of the classical FK model for these values of β. Thus, the existence of supersonic kink velocities could be considered as a solely dynamical effect, i.e., the anharmonicity of the interatomic interaction leads to a change of the character of kink's motion from the SG-like to the Toda-like type.

When the driving force increases above the PN value, f_{PN}, the kink begins to move and radiate phonons due to the discreteness effects. The radiation increases with kink velocity (e.g., see the shape of the supersonic kink in Fig. 5), and finally this radiation leads to kink decay. Note that although the kink velocity essentially depends on the anharmonicity parameter β, the $v_{\mathrm{kink}}(f)$ dependence remains qualitatively

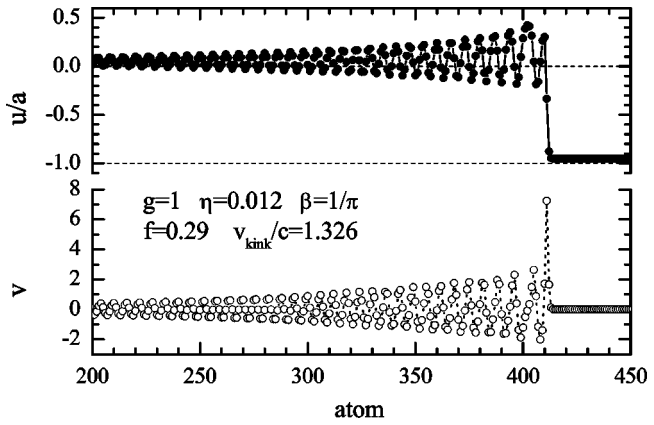

FIG. 5. Shape of the single kink just prior to its decay for $\beta = 1/\pi$, $g = 1$, and $\eta = 0.012$.

the same for all values of β shown in Fig. 3.

When the force exceeds the critical value f_{1r}, the scenario of kink's decay for low values of the anharmonicity parameter β is similar to that of the classical FK model described in detail in Ref. [10] as shown in Fig. 6. The primary kink generates new kink-antikink pairs. The newly created antikinks also generate the kink-antikink pairs, and the collisions of these kinks and antikinks lead to the transition to the running state.

The kinetics of the kink decay at large values of the anharmonicity β is different. As one can see from Fig. 7, now a new kink-antikink pair is created not just behind the primary kink, but at some distance (about ten lattice constants) from the kink center. Recall that the main effect of anharmonicity is the violation of the kink-antikink symmetry (e.g., see Ref. [1], and references therein): when $\beta > 0$, the antikink moves more slowly than the kink. At $f = f_{1r}$, the antikink is unstable and generates new kink-antikink pairs. This process finally results in the transition of the whole system to the running state.

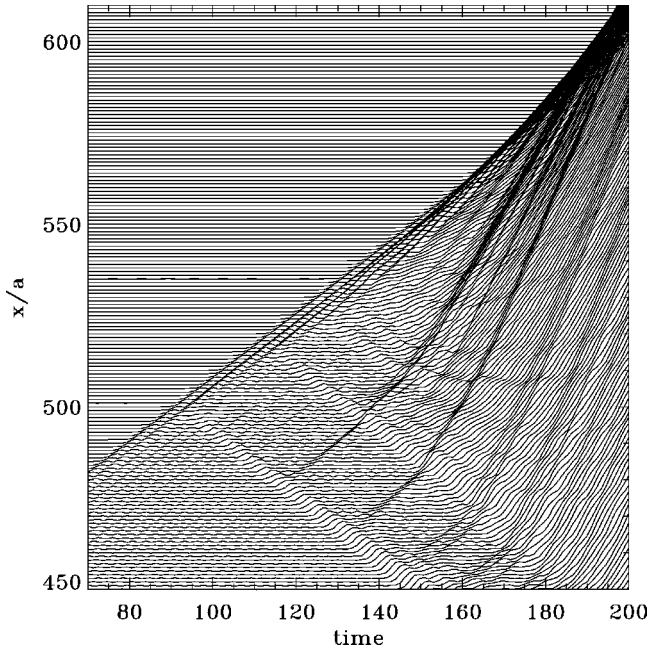

FIG. 6. Destruction of the single kink for $\beta = 0.01$, $g = 1$, $\eta = 0.012$, and $f = 0.425$. The initial configuration corresponds to the steady kink motion at $f = 0.423$. The transition to the running state begins just after the first kink-antikink collision.

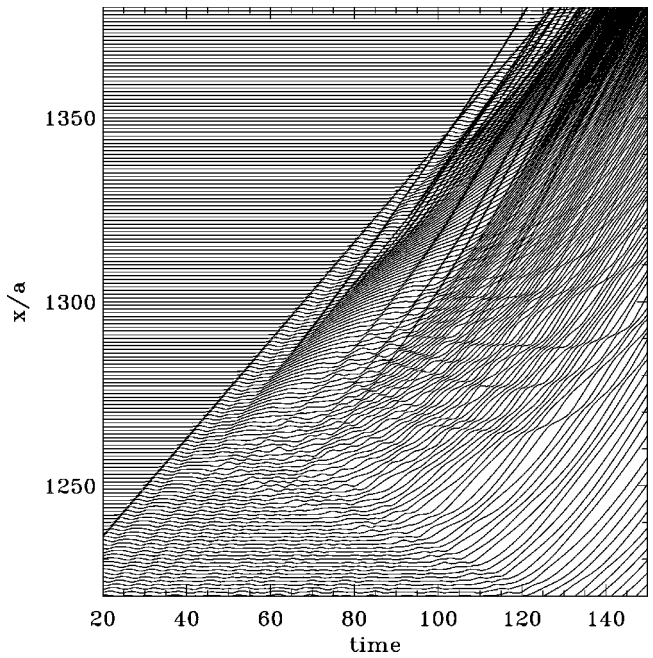

FIG. 7. Decay of the single kink for $\beta = 1/\pi$, $g = 1$, $\eta = 0.012$, and $f = 0.295$. The initial configuration corresponds to the steady kink motion at $f = 0.29$. A new kink-antikink pair is created in the tail of the moving kink at a distance $\sim 10a$ from the primary kink.

B. Double kink

The force-velocity characteristics of the double kink for different values of the anharmonicity parameter β are presented in Fig. 8. In these simulations, we first found the steady-state moving kink configuration somewhere at the middle of the stability interval starting from the Toda kink shape, and then adiabatically increased and decreased the dc force. The kink shape for different values of β, was also obtained one from another by adiabatic change of this parameter. One can see that at low β, the double kink exists for a very narrow interval of velocities. For example, for $\beta = 0.01$, the double kink moves with almost a fixed velocity $v_{\mathrm{kink}} \approx 0.85\,c$. Recall that in the undamped discrete SG model without driving, the double kink can exist with a fixed velocity $v_{\mathrm{kink}} \approx 0.82\,c$ only [6]. In the model under study, we have to apply a dc force to compensate for energy loss due to the external damping. The instantaneous profile of the double kink for $\beta = 0.01$ is shown in Fig. 9. The kink shape is smooth at the left boundary of the stability interval [Fig. 9(a)]. When f increases, the kink begins to radiate in order to compensate for the increase of the force over the f_{2l} value. The radiation increases with f [see Fig. 9b], and finally at $f = f_{2r}$ the double kink collapses.

When the anharmonicity parameter β increases, the interval of allowed kink's velocities increases too. For example,

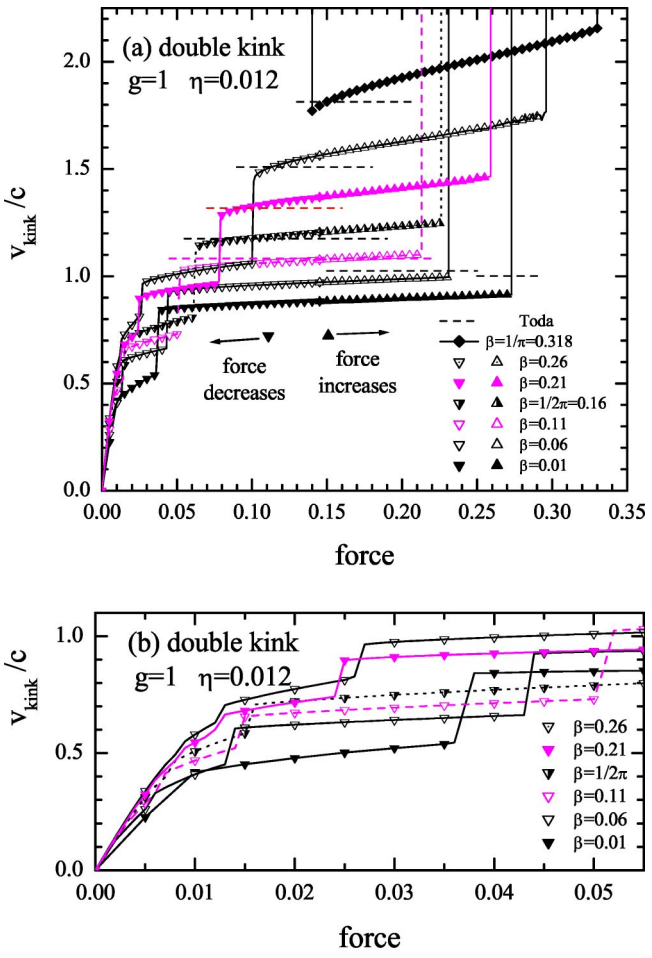

FIG. 8. (a) Velocity v_{kink}/c vs f for the double kink for different values of the anharmonicity parameter β as indicated in the legend ($g=1$ and $\eta=0.012$). The dash horizontal lines show the velocity of the corresponding Toda soliton. Panel (b) shows the $v_{\mathrm{kink}}(f)$ dependencies at low forces. The jumps correspond to splitting of the double kink into two single kinks separated by one, two, etc., lattice constants.

for $\beta=1/\pi$, the velocity of the double kink may take values within the interval $1.77<v_{\mathrm{kink}}/c<2.16$. The kink's shape for this case is shown in Fig. 10. One can see that when the double kink moves with a velocity close to the Toda velocity $v_{\mathrm{Toda}}\approx 1.81\,c$, its shape is smooth [Fig. 10(b)], i.e., the kink moves almost without radiation. But when the kink velocity deviates from the Toda value, the double kink begins to radiate and finally decays.

In the example described above, where the damping $\eta=0.012$ was used, the value of the Toda velocity was very close to the left boundary of the stability interval. When the damping is larger, e.g., $\eta=0.05$, the velocity v_{Toda} is at the middle of the interval of the velocities allowed for the double kink, and now oscillations of the kink shape are very large both at the left and at the right boundaries as shown in Fig. 11.

The double kink can exist in the moving state only. When the force is turned off, the double kink splits into two separate single kinks as illustrated in Fig. 12. The double kink leaves a single kink behind itself, which then quickly stops,

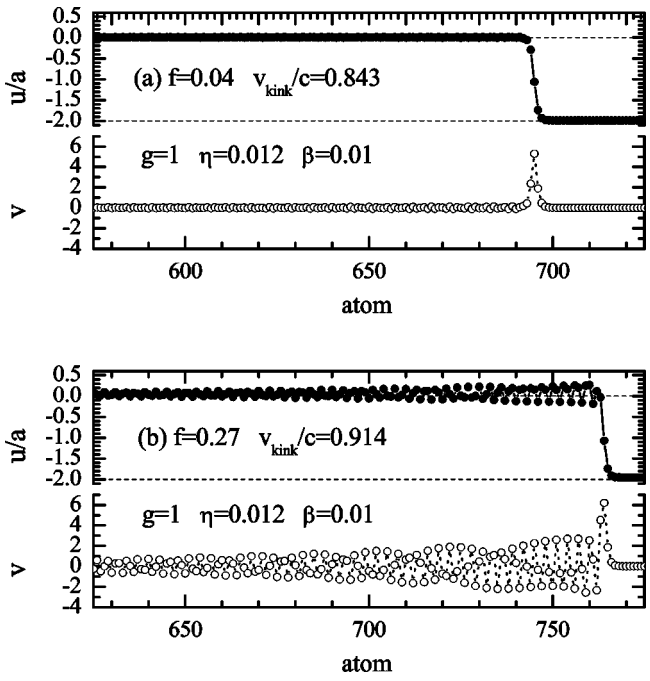

FIG. 9. Shape of the double kink for $\beta=0.01$, $\eta=0.012$, and $g=1$ at (a) the left boundary ($f=0.04$, $v_{\mathrm{kink}}/c=0.843$) and (b) the right boundary ($f=0.27$, $v_{\mathrm{kink}}/c=0.914$).

while the ahead single kink continues to move over a distance $\sim v_{\mathrm{Toda}}/\eta$.

A similar behavior is observed when the force decreases adiabatically. At $f=f_{2l}$ the double kink splits into two single kinks separated by one lattice constant, and the velocity jumplike decreases [see Fig. 8(b)]. With further decrease of f, the distance between the single kinks jumplike increases (each time on one lattice constant) and simultaneously the velocity decreases until both kinks stop. The same scenario was observed by Ustinov *et al.* [5] in the classical FK model. In the anharmonic model, however, such a scenario is observed for low values of the anharmonicity parameter only (e.g., for $\beta<0.3$ in the case of $g=1$). For a large β, for example, for the case of $\beta=1/\pi$ shown in Fig. 13, the scenario is different. The double kink becomes unstable and emits antikinks, while newly created kinks move together with the primary kink (creating a "traffic jam" discussed in detail in Ref. [9]). The total velocity of the system grows approximately linearly with time, and finally the whole system goes to the running state.

The scenarios described above are typical for the kink decay. However, for some sets of the model parameters, we also observed a more complicated kinetics of the decay. For example, in the case of a smaller value of the elastic constant, $g=0.5$, the double kink transforms into the triple kink and the single antikink during the force decreasing process at $f=f_{2l}$ (see Fig. 2). Then, with further decrease of the force, at $f=0.01$, the triple kink annihilates with the single antikink so that the system leaves with two single kinks. One more example of a nontrivial scenario of the kink decay will be described below for the case of the triple kink.

Finally, let us describe the mechanism of kink decay when the force adiabatically increases above the stability interval.

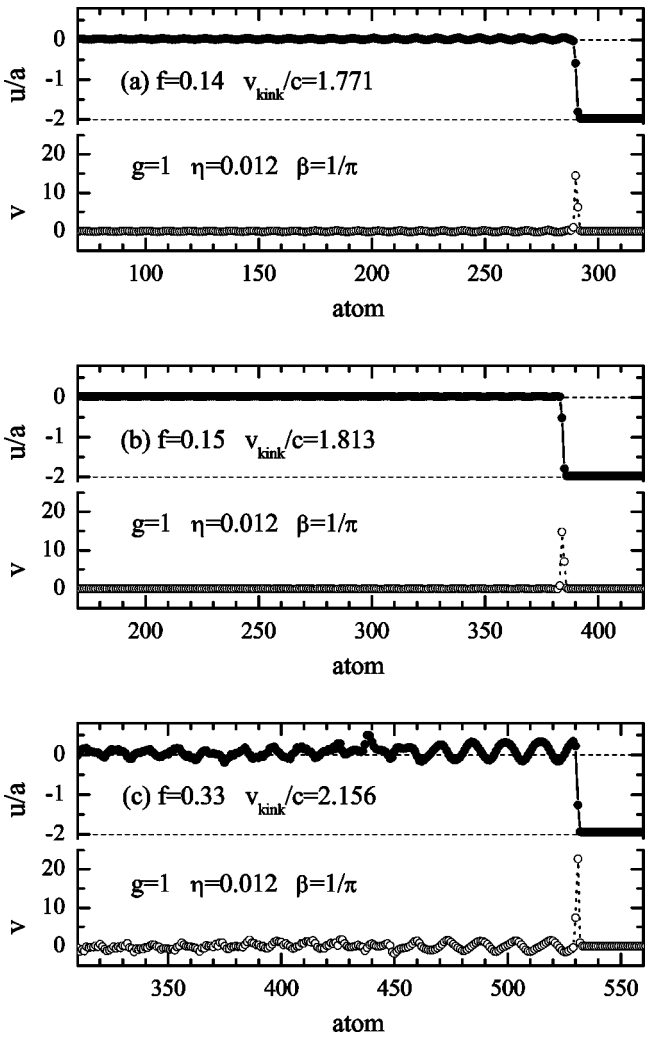

FIG. 10. Shape of the double kink for $\beta=1/\pi$, $\eta=0.012$, and $g=1$ for different forces: (a) at the left boundary ($f=0.14$, $v_{\mathrm{kink}}/c=1.771$), (b) $f=0.15$ when $v_{\mathrm{kink}}/c=1.813\approx v_{\mathrm{Toda}}/c$, and (c) at the right boundary ($f=0.33$, $v_{\mathrm{kink}}/c=2.156$).

At low anharmonicity parameter β, the scenario is similar to that of the single kink (e.g., see Fig. 14 for the case of $\beta=0.01$ and compare it with Fig. 6). The primary kink emits new kink-antikink pairs, then the antikinks also emit new kink-antikink pairs, and the collisions of kinks with antikinks result in the transition to the running state. At large values of the anharmonicity parameter β, the scenario, however, is different. Now a new kink-antikink pair is created far away from the primary kink, e.g., at a distance $\sim 100a$ as shown in Fig. 15. Then, the newly created kink generates new kink-antikink pairs, and this finally results in the transition to the running state. Note that close to the instability threshold, the kink's shape is irregular [see Fig. 10(c)]. Note also that at higher values of the damping constant the scenarios are similar, although the distance, where the new kink-antikink pair is created, is now shorter (e.g., $\sim 10a$ for $\eta=0.05$).

C. Triple kink

Properties of the triple kink are in many aspects similar to those of the double kink. The $v_{\mathrm{kink}}(f)$ dependencies for the triple kink for different values of the anharmonicity β are summarized in Fig. 16. In the limit $\beta\to 0$, the triple kink exists only for an approximately constant velocity in agreement with the Champneys and Kivshar result [6] for the undamped undriven classical FK model. For example, for $\beta=0.01$, the velocity of the triple kink lies within the very narrow interval $0.9<v_{\mathrm{kink}}/c<0.94$. At larger values of the anharmonicity, parameter $\beta>0.1$, the kink velocity changes with force, but remains within a narrow interval around the Toda velocity (6).

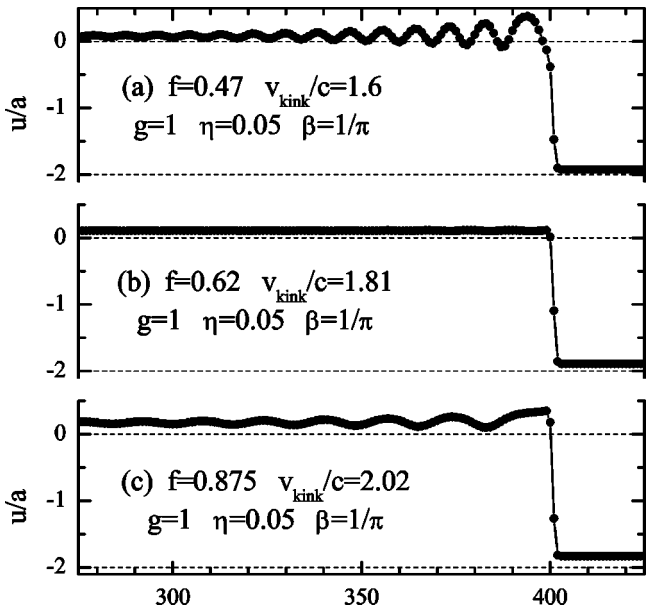

FIG. 11. Shape of the double kink for $\beta=1/\pi$, $g=1$, and $\eta=0.05$ for different values of the force: (a) close to the left boundary, (b) when the kink velocity is close to the Toda velocity, and (c) close to the right boundary.

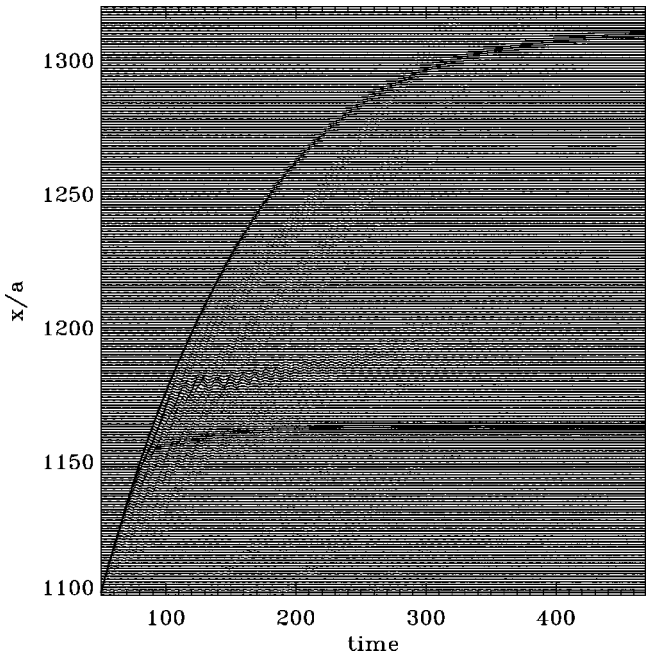

FIG. 12. Free evolution of the double kink for the parameters $g=1$, $\beta=1/\pi$, and $\eta=0.012$.

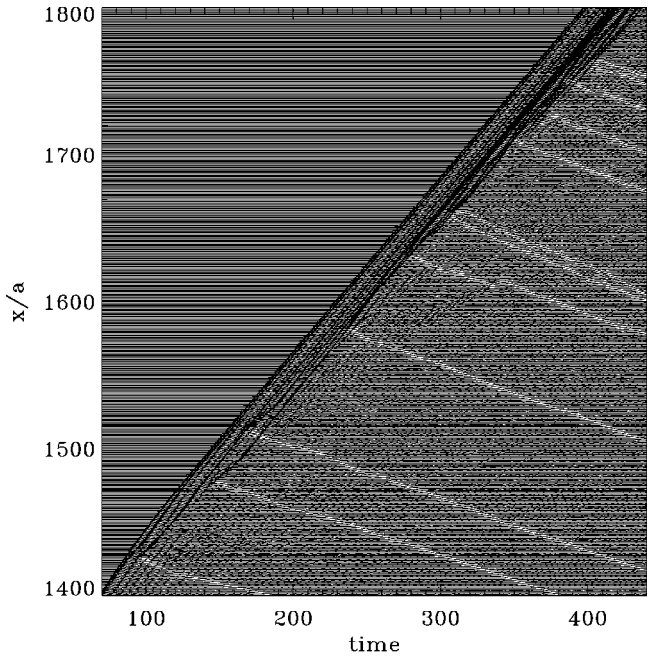

FIG. 13. Decay of the double kink for the $\beta=1/\pi$ case when the force decreases adiabatically ($f=0.13$, $g=1$, and $\eta=0.012$; the initial configuration corresponds to the steady kink motion at $f=0.14$).

The shape of the triple kink is shown in Fig. 17 for a nearly harmonic model, $\beta=0.01$, and in Fig. 18 for a large value of the anharmonicity parameter $\beta=1/\pi$. In the former case, the radiation is low at the left boundary $f=f_{3l}$ and

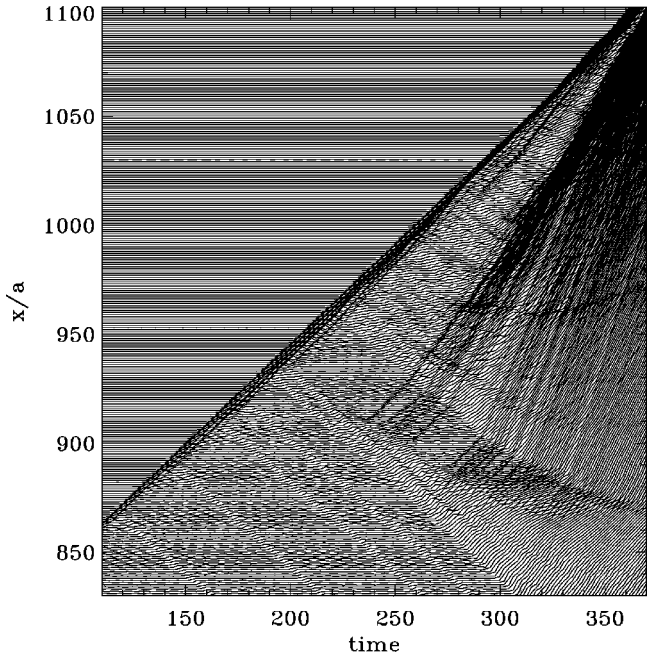

FIG. 14. Decay of the double kink when the force adiabatically increases above the stability interval for the case of small anharmonicity parameter $\beta=0.01$ ($f=0.275$, $g=1$, and $\eta=0.012$; the initial configuration corresponds to the steady kink motion at $f=0.273$).

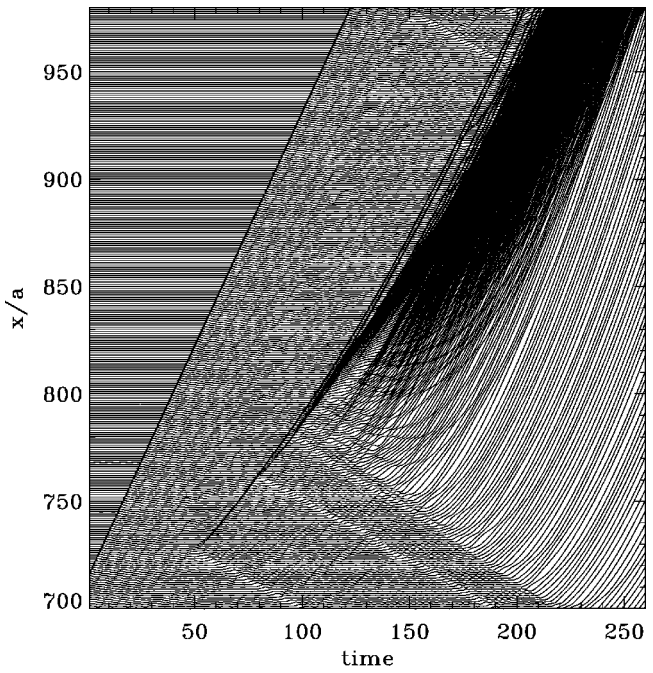

FIG. 15. The same as Fig. 14, but for large anharmonicity parameter $\beta=1/\pi$ ($f=0.34$, the initial configuration corresponds to the steady kink motion at $f=0.33$).

increases with force growing until the kink becomes unstable and decays at $f=f_{3r}$. In the case of $\beta=1/\pi$, the radiation is low when the kink velocity is at the middle of the stability interval, and increases when the kink velocity deviates from the Toda value to lower or higher values. Again, note that, close to the boundaries of the stability interval, the oscillations in the kink's tail are irregular.

Analogously to the double kink, the triple kink can exist in the moving state only. When the force is turned off, the

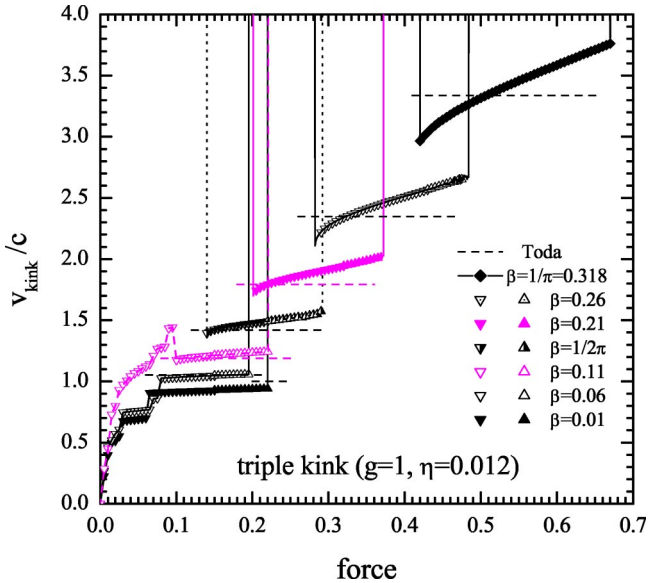

FIG. 16. $v_{\mathrm{kink}}(f)/c$ for the triple kink for different values of the anharmonicity parameter β as shown in the legend ($g=1$ and $\eta=0.012$). The dashed horizontal lines show the velocities of the corresponding Toda soliton.

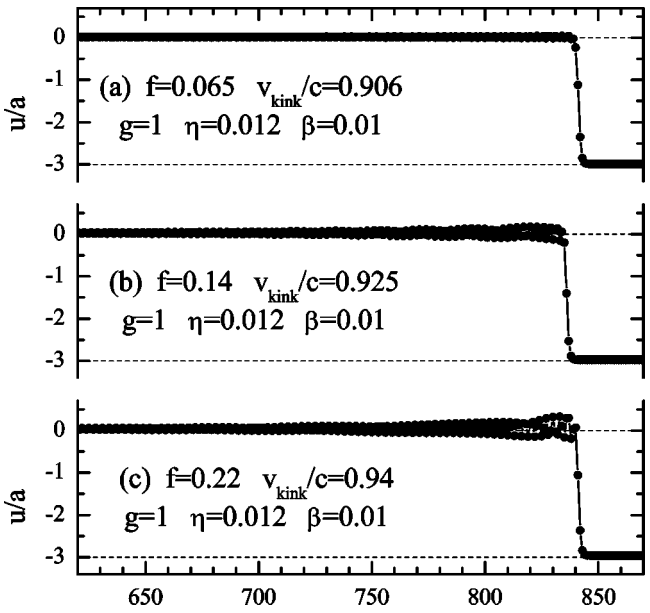

FIG. 17. Shape of the triple kink for $\beta=0.01$ for three values of the dc force: (a) close to the left boundary, (b) at the middle of the stability interval, and (c) close to the right boundary ($g=1$ and $\eta=0.012$).

triple kink splits into single kinks leaving them behind itself. When the force is decreased adiabatically, the triple kink becomes unstable at $f=f_{3l}$. At low anharmonicity parameter, e.g., $\beta<0.11$ for $g=1$, the triple kink leaves a single kink behind itself; the ''ahead'' double kink also soon splits into two single kinks separated by one lattice constant, and the further scenario is similar to that described above for the case of the double kink. However, in the highly anharmonic

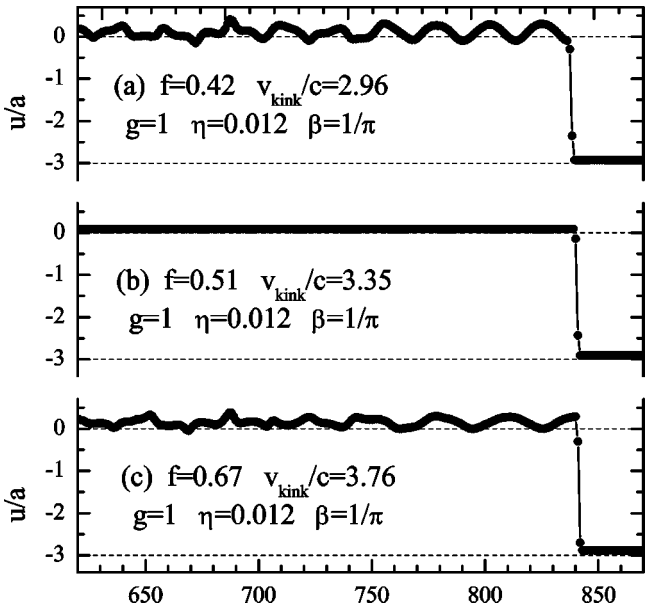

FIG. 18. Shape of the triple kink for $\beta=1/\pi$ for three values of the force: (a) close to the left boundary, (b) when the kink velocity is close to the Toda velocity, and (c) close to the right boundary ($g=1$ and $\eta=0.012$).

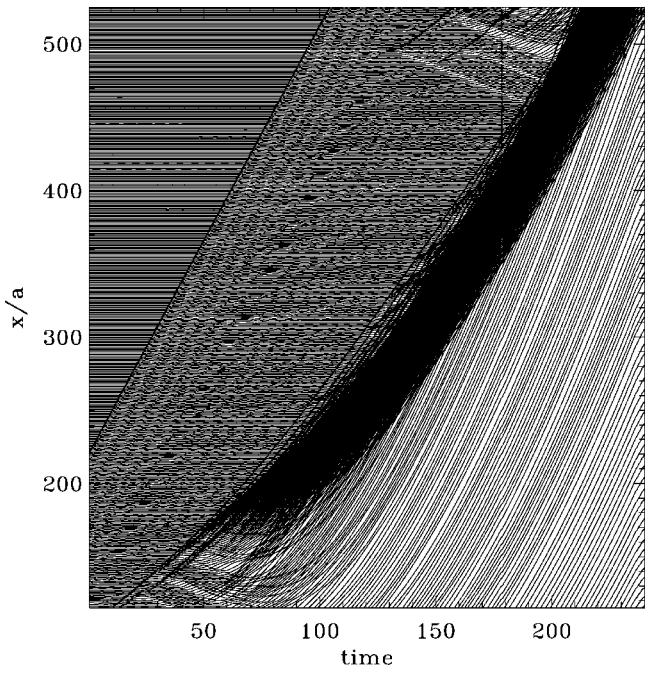

FIG. 19. Decay of the triple kink in the anharmonic model for adiabatically decreasing force ($\beta=1/\pi$, $f=0.415$, $g=1$, and $\eta=0.012$; the initial configuration corresponds to the steady kink motion at $f=0.42$).

model, e.g., when $\beta>0.11$ for the $g=1$ case, the system goes to the running state according to the scenario shown in Fig. 19. Now new kink-antikink pairs are generated in the kink's tail far away from the primary moving kink (at a distance $\gtrsim 100a-200a$ for the parameters used in Fig. 19), and this stimulates the transition of the whole system to the running state.

An interesting scenario was observed for the ''intermediate'' $\beta=0.11$ case. When the force is decreased adiabatically, at $f=0.095$ the triple kink splits into a double kink ($2k$) and a single kink. The single kink almost immediately generates in its tail a new kink-antikink pair. The newly created kink and the old single kink are coupled together into a $2k^+$ kink (two single kinks separated by one lattice constant), so that there are two double kinks ($2k$ and $2k^+$) and one antikink in the system at this stage of system evolution. The $2k^+$ kink moves slightly slower than the $2k$ kink. All collisions between these kinks are ''elastic.'' With further decrease of the force, the antikink and the double kink annihilate during their collision thus creating a single kink, so that the system has one single kink and one $2k^+$ kink in the result. Then, the $2k^+$ kink overtakes the single kink, these join together and move as one complex. With further decrease of f, the distance between single kinks in the $2k^+$ kink begins to increase, and finally all three single kinks stop.

Finally, when the force is increased above the stability interval, the triple kink collapses and stimulates the transition of the whole system to the running state as well. The kinetics of this transition is slightly different at low and large values of the anharmonicity parameter β. For example, at $\beta=0.01$, the triple kink generates kink-antikink pairs just behind itself. The antikinks move to the left (against the force),

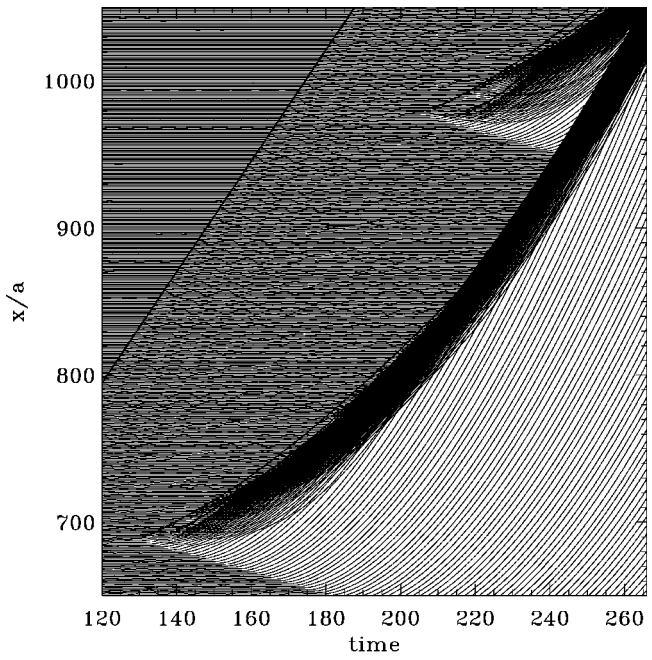

FIG. 20. Scenario of destruction of the triple kink in the anharmonic model for the force increasing process ($\beta=1/\pi$, $f=0.675$, $g=1$, and $\eta=0.012$; the initial configuration corresponds to the steady kink motion at $f=0.67$).

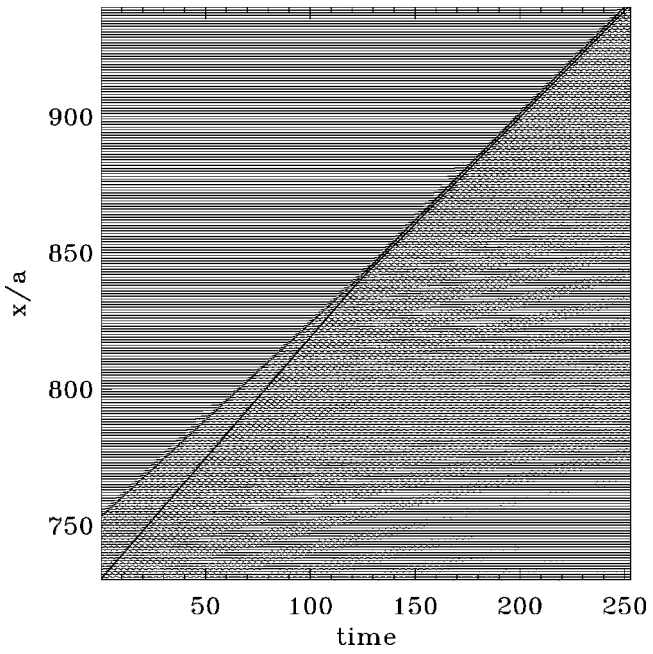

FIG. 21. Collision of the double kink and the single kink in the nearly harmonic model ($\beta=0.01$, $f=0.15$, $g=1$, and $\eta=0.012$).

while the kinks join together increasing the topological charge of the primary kink. The moving antikinks generate kink-antikink pairs as well, and collisions of newly created kinks and antikinks result in the transition to the running state. This scenario is similar to that for the single kink and double kink described above. On the other hand, at a high anharmonicity of the interaction, e.g., for the case of $\beta=1/\pi$ shown in Fig. 20, the scenario of the transition reminds us that for the case the force decreasing process (compare Figs. 20 and 19). Now new kink-antikink pairs are generated far away from the primary kink (at a distance $\gtrsim 200\,a$), and this stimulates the transition of the whole system to the running state.

D. Kink collisions

In the preceding sections, we considered the cases where there was only one kink in the system. Now let us discuss the evolution of the system with several kinks. If all kinks are of the same topological charge, these all move with the same velocity in the steady state and, therefore, these cannot collide.

However, due to overlapping of the stability intervals, the system may contain kinks of different topological charges simultaneously, for example, a single kink and a double kink. Because the single and double kinks are characterized by different velocities at a given value of the dc force, they must collide after some time. The result of such a collision depends on the driving force f and on the anharmonicity parameter β. For example, in the case of nearly harmonic interaction between the atoms, $\beta=0.01$, the collision results in the formation of a triple kink as shown in Fig. 21. Because the triple kink is stable at the given value of the force, it moves without further changes.

Moreover, when the system contains one double kink and several single kinks, the double kink, having a higher velocity, will overtake the single kinks one by one, increasing its own topological charge. However, the kink topological charge p cannot grow infinitely—when p reaches some critical value, the kink becomes unstable. For example, Fig. 22 shows the system configuration when the double kink already overtook three single kinks and reached the topological charge $p=5$. After that the $p=5$ kink becomes unstable, it begins to emit antikinks, and the next collision with a single kink results in the transition to the running state as shown in Fig. 23.

In the highly anharmonic model, the transition to the running state begins much earlier. For example, in the case of $\beta=1/\pi$, already the first collision of the double and single kinks results in the transition to the running state as demon-

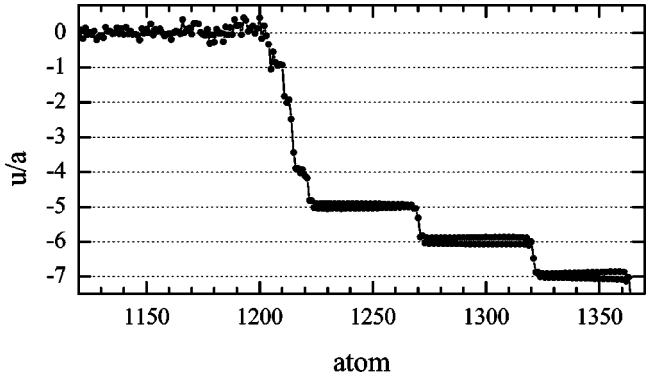

FIG. 22. The system configuration after creation of the $p=5$ kink ($\beta=0.01$, $f=0.15$, $g=1$, and $\eta=0.012$).

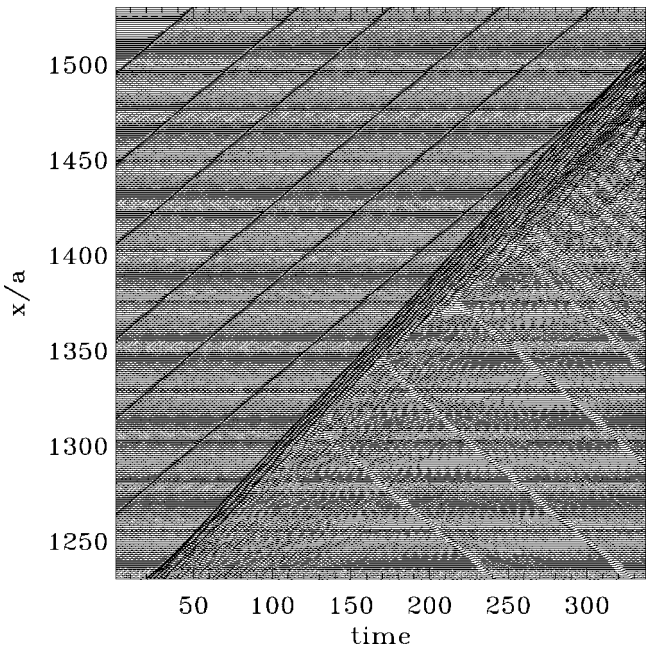

FIG. 23. Collision of the $p=5$ kink with the single kink ($\beta=0.01$, $f=0.15$, $g=1$, and $\eta=0.012$).

strated in Fig. 24. In this case, the stability intervals of the double and triple kinks do not overlap, so that the triple kink is unstable at this value of the force.

III. DISCUSSION

As we mentioned already in Sec. II, the stability of the multiple kink in the anharmonic FK model is determined

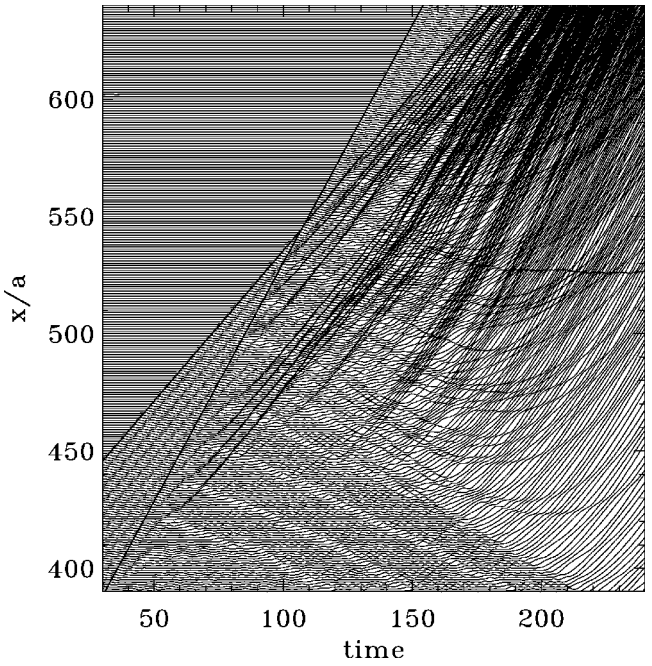

FIG. 24. Collision of the double kink and the single kink in the highly anharmonic model ($\beta=1/\pi$, $f=0.25$, $g=1$, and $\eta=0.012$).

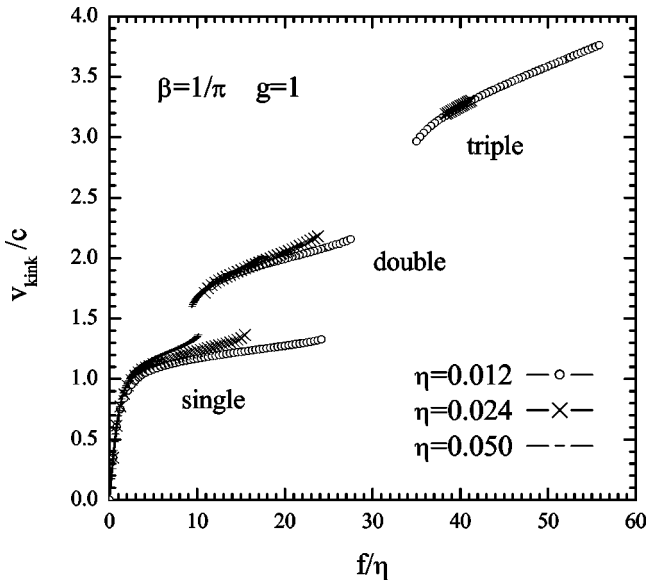

FIG. 25. Dependence v_{kink}/c vs f/η for the single, double, and triple kinks for three different values of the damping constant: $\eta=0.012$, 0.024, and 0.05 ($\beta=1/\pi$ and $g=1$).

mainly by its velocity. Indeed, if we replot the data from Fig. 1 in the coordinates v_{kink}/c versus f/η (see Fig. 25), then the ''scaled'' force-velocity dependencies for different values of the damping constant η almost coincide, especially at left-hand parts of the stability intervals.

If the value of the driving force f is kept fixed, then the kink velocity v_{kink} monotonically increases with the anharmonicity parameter β as shown in Fig. 26. When the anharmonicity exceeds a certain value, e.g., $\beta>0.1$ for the $g=1$ case, v_{kink} becomes close to the Toda velocity v_{Toda}. In the highly anharmonic FK model, the multiple kinks can exist

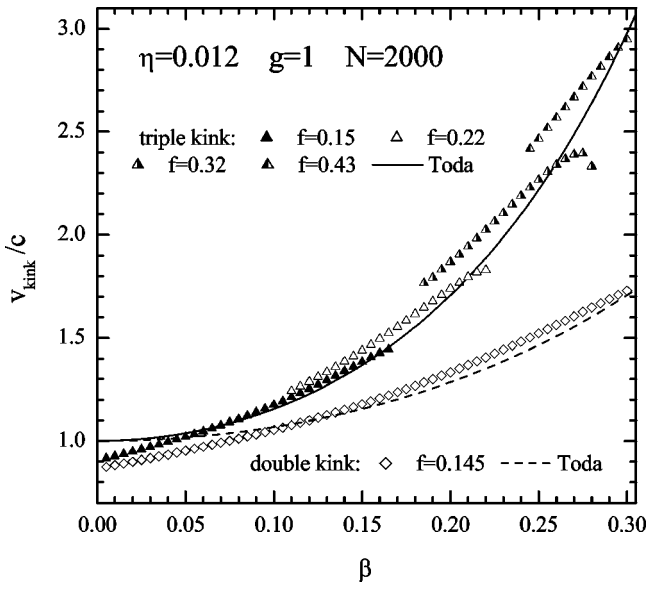

FIG. 26. Dependence of the velocties v_{kink}/c of the double and triple kinks on the anharmonicity parameter β at a fixed value of the dc force (shown in the legend) for $g=1$ and $\eta=0.012$.

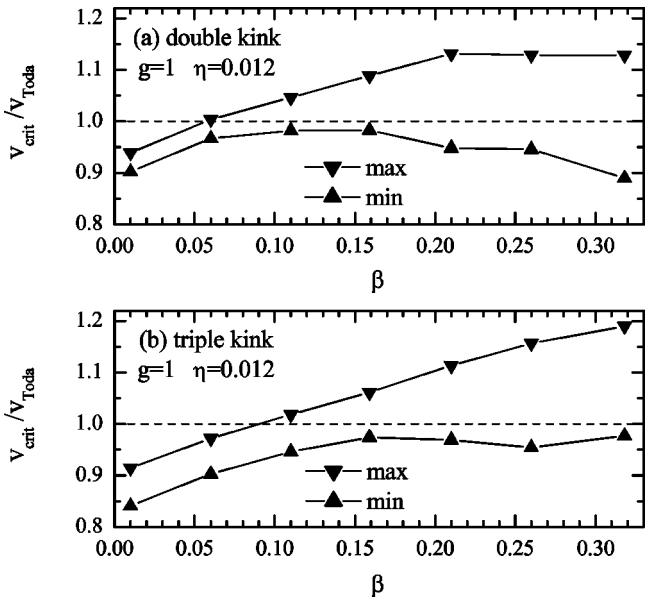

FIG. 27. Critical velocities $v_{\mathrm{crit}}/v_{\mathrm{Toda}}$ of the double and triple kinks as functions of the anharmonicity parameter β for $g=1$ and $\eta=0.012$.

only with supersonic velocities close to those of the corresponding Toda soliton.

Thus, for a large enough degree of the anharmonicity of the interatomic interaction, e.g., $\beta>0.1$ for $g=1$, the behavior of the multiple kinks should remind us that of the Toda soliton. The multiple kink is stable for forces within the interval $f_{pl}<f<f_{pr}$, and its velocity monotonically increases with f within a nonzero interval $v_{p,\,\min}<v_{\mathrm{kink}}<v_{p,\,\max}$. The critical values of the kink velocity as functions of the anharmonicity parameter β are plotted in Fig. 27. One can see that the width of the interval of the allowed kink's velocities increases with β, and the Toda velocity lies inside the stability interval for $\beta>0.1$. When the kink velocity is close to v_{Toda}, it moves almost without radiation. But when the kink velocity deviates from the Toda one, it begins to radiate phonons into its own tail and finally collapses.

The whole dependence $v_{\mathrm{kink}}(f)$ for the multiple kink may, in principle, be found from the force balancing arguments. In the steady state, the driving force must be compensated by the total frictional force, $f=m_p\eta_{\mathrm{eff}}v_{\mathrm{kink}}$, where m_p is the effective kink's mass and $\eta_{\mathrm{eff}}=\eta+\eta_{\mathrm{int}}$ is the total damping experienced by the kink, which consists of the external damping η and an additional damping η_{int} emerging due to radiation of phonons. The mass m_p can be calculated from the kink's shape through the integral (e.g., see Ref. [16] and also Ref. [1], and references therein) $m_p=a^{-1}\int_{-\infty}^{+\infty}dz[u'(z)]^2$. The kink's shape can be found, for example, with the help of the variational method developed in Ref. [11] as a proper combination of the SG kink shape (1) and the Toda soliton shape (5) with some fitting parameters. Even if we ignore the radiational losses η_{int}, the described approach leads to a qualitative correct dependence $v_{\mathrm{kink}}(f)$ [11].

However, in order to get a quantitative agreement with the simulation results, one should calculate analytically the losses due to phonon radiation, which is the most difficult problem [17]. Although there are methods to estimate η_{int} (e.g., see Ref. [1], and references therein), these are too complicated and the achieved accuracy is typically not too satisfactory. Besides, such an approach cannot predict the stability intervals of multiple kinks. As was shown in Ref. [10], the instability of the fast kink is in fact a delicate problem, the kink becomes unstable due to the excitation of an internal kink's localized mode in its tail. Thus, a direct simulation of the dependence $v_{\mathrm{kink}}(f)$ still remains a more straightforward approach to the problem.

IV. CONCLUSION

Thus, we have presented the detailed numerical study of multiple kinks in the driven anharmonic FK model. We showed that multiple kinks with a topological charge $p\geqslant 2$ do exist in the *discrete* model in accordance with the results of the previous works. These kinks cannot be static, they are stable in the moving state only.

At low anharmonicity of the interatomic interaction, when the dimensionless anharmonicity parameter βa is lower than 0.5, the multiple kinks move with a subsonic velocity v_{pm}. The value of this velocity is in agreement with that calculated analytically in Ref. [6]. The kink velocity is almost independent of the external driving *f*. The interval of forces, where the multiple kink is stable, is determined by $f_{pl}\approx m_p\eta v_{pm}$ from the left-hand side (the force must compensate energy loss due to the external damping), while from the right-hand side the kink stability is destroyed due to increasing of phonon radiation, which emerges in order to compensate the energy $\propto(f-f_{pl})$ pumped into the system by the driving. When the force is outside the stability interval, the multiple kink decays. At low forces, $f<f_{pl}$, the multiple kink typically splits into several kinks with lower topological charges. This process proceeds through intermediate stages, where separation between the child kinks increases by steps. At high forces, $f>f_{pr}$, the multiple kink becomes unstable and emits kink-antikink pairs behind itself. The newly created antikinks move against the force with approximately the same velocity due to kink-antikink symmetry and emit kink-antikink pairs as well. Then, collisions of kinks and antikinks lead to the transition of the whole system to the running state. Note that this scenario is approximately the same for the single $(p=1)$ kink as well [10].

In a highly anharmonic FK model, when $\beta a>0.5$, the multiple kinks are supersonic, and their properties are close to those of the Toda soliton. Now a range of allowed kink's velocities is much larger than in the classical FK model, and the value of v_{kink} monotonically increases with *f*. When the kink velocity is close to that of the corresponding Toda soliton, i.e., at $f\approx m_p\eta v_{\mathrm{Toda}}$, the multiple kink moves almost without radiation. But when the kink velocity deviates from this value (either to lower or to higher values), the kink begins to radiate phonons and finally becomes unstable. The scenario of kink's destruction is different from that of the classical FK model. Now the kink's tail becomes irregular, and new kink-antikink pairs are generated far away from the primary kink. The creation of these kink-antikink pairs leads

to the transition of the whole system to the running state. At low damping, e.g., at $\eta=0.012$, the new kink-antikink pairs are emerged at a distance of about ten lattice constants from the primary kink in the case of the 2π kink, at about 100 lattice constants for the double kink, and at $>200a$ in the case of the triple kink. When the damping constant is larger, the kink's tail is shorter and these distances are smaller too.

It is important to note that multiple kinks with a topological charge $p\geqslant 2$ may only be observed in a system with a low enough damping η, because the driven kink has to reach a high velocity $v_{\mathrm{kink}}\sim v_{\mathrm{Toda}}$ at forces $f<1$, i.e., before that the minima of the substrate potential disappear. Note also that in the simulation of the driven anharmonic FK model, we did not observe the hierarchy of multiple kink states predicted in Refs. [14,15], probably, because we always started from the monotonic (either SG or Toda) kink shape.

Typically a system may contain either one multiple kink or several kinks of the same topological charge p (a train of multikinks), which all move with the same velocity. When the kinks of different topological charges are present in the system simultaneously (this is possible if their stability intervals overlap), these kinks will move with different velocities and must collide after some time. Such a collision is typically destructive and leads to the transition of the whole system to the running state. For example, even when the single and double kinks are united into a triple kink after the collision as was observed in the case of $\beta=0.01$ (see Fig. 21), next collisions of the triple kink (whose velocity is the largest one in the system) with other kinks will finally destroy the steady state.

The effect described above leads to an interesting conclusion that at a nonzero temperature T, the system of single kinks should be unstable at forces $f>f_{2l}$ even if the 2π kinks are still stable at the given force, $f<f_{1r}$. Indeed, at $T>0$ the kink's velocities fluctuate, so that some of the kinks may collide and form a double kink. Besides, double kinks may also be created due to thermal fluctuations. Then, the double kink will move faster than other single kinks. Therefore, it will overtake the single kinks one by one, finally destroying the steady state. However, the described scenario operates in the *infinite* system only. In a finite-length chain, where the probability of thermal excitation of new kink-antikink pairs is negligible at low enough temperature, all results of the present work should be valid as has been mentioned in Ref. [11]. Note that at lower forces, $f<f_{2l}$, the single kinks in the anharmonic FK model should come close to each other creating a ''traffic jam'' state [9].

Note also that while the 2π kinks can be smoothly accelerated up to supersonic velocities starting from the static configuration, the multiple kinks with $p\geqslant 2$ have to be launched into the system artificially with already correct shape and velocity, e.g., from a free end of the chain, because these cannot exist in the static state.

The supersonic and multiple kinks discussed in the present paper may have applications in the different physical systems already mentioned in the Introduction. In particular, the instability of fast kinks is responsible for the sharp transition from the low-mobility motion to the high-mobility sliding state and the hysteresis in driven systems. Although we do not know experimental situations, where these types of excitations were directly observed, molecular dynamics (MD) simulation of dislocation dynamics in two-dimensional (2D) systems exhibits some features discussed in the present work. In particular, Gumbsch and Gao [18] observed a supersonic propagation of dislocations. Also, Pouget *et al.* [19] and recently Gornostyrev *et al.* [20] have observed in MD simulation of the 2D FK model the nucleation of kink-antikink pairs in the tail of the moving dislocation under the applied (strong enough) stress. It was noted that such an effect may lead to a nontrivial temperature dependence of yield stress in metals and alloys with a sufficiently high PN relief.

ACKNOWLEDGMENTS

Discussions with F. Marchesoni and M. Peyrard are gratefully acknowledged. The work of O.B. was supported in part by NATO Grant No. HTECH.LG 971372 and INTAS Grant No. 97-31061, and that of H.Z., B.H., and J.T. by grants from the Hong Kong Research Grants Council (RGC) and the Hong Kong Baptist University Faculty Research Grant (FRG).

[1] O.M. Braun and Yu.S. Kivshar, Phys. Rep. **306**, 1 (1998).
[2] M. Peyrard and M.D. Kruskal, Physica D **14**, 88 (1984).
[3] A.V. Savin, Y. Zolotaryuk, and J.C. Eilbeck, Physica D **138**, 267 (2000).
[4] B.A. Malomed, Phys. Rev. B **41**, 2616 (1990).
[5] A.V. Ustinov, B.A. Malomed, and S. Sakai, Phys. Rev. B **57**, 11 691 (1998).
[6] A. Champneys and Yu.S. Kivshar, Phys. Rev. E **61**, 2551 (2000).
[7] O.M. Braun, T. Dauxois, M.V. Paliy, and M. Peyrard, Phys. Rev. Lett. **78**, 1295 (1997); Phys. Rev. E **55**, 3598 (1997); M. Paliy, O. Braun, T. Dauxois, and B. Hu, *ibid.* **56**, 4025 (1997).
[8] O.M. Braun, A.R. Bishop, and J. Röder, Phys. Rev. Lett. **79**, 3692 (1997).
[9] O.M. Braun, B. Hu, A. Filippov, and A. Zeltser, Phys. Rev. E **58**, 1311 (1998).
[10] O.M. Braun, B. Hu, and A. Zeltser, Phys. Rev. E **62**, 4235 (2000).
[11] O.M. Braun, Phys. Rev. E **62**, 7315 (2000).
[12] M. Toda, J. Phys. Soc. Jpn. **22**, 431 (1967); **23**, 501 (1967); *Theory of Nonlinear Lattices* (Springer-Verlag, Berlin, 1981).
[13] A.R. Bishop, D.K. Campbell, P.S. Lomdahl, B. Horovitz, and S.R. Phillpot, Synth. Met. **9**, 223 (1984).
[14] A.V. Savin, Zh. Éksp. Teor. Fiz. **108**, 1105 (1995) [JETP **81**, 608 (1995)].
[15] Y. Zolotaryuk, J.C. Eilbeck, and A.V. Savin, Physica D **108**, 81 (1997).

[16] C. Cattuto, G. Costantini, T. Guidi, and F. Marchesoni, Phys. Rev. B **63**, 094308 (2001).
[17] C. Cattuto, G. Costantini, T. Guidi, and F. Marchesoni, Phys. Rev. E **63**, 046611 (2001).
[18] P. Gumbsch and H. Gao, J. Comput.-Aided Mater. Des. **6**, 137 (1999); Science (Washington, DC, U.S.) **283**, 965 (1999).
[19] J. Pouget, S. Aubry, A.R. Bishop, and P.S. Lomdahl, Phys. Rev. B **39**, 9500 (1989).
[20] Yu.N. Gornostyrev, M.I. Katsnelson, A.V. Kravtsov, and A.V. Trefilov, e-print cond-mat/0206428.